

# SCIENTIFIC REPORTS



OPEN

## TSPO ligand residence time: a new parameter to predict compound neurosteroidogenic efficacy

Barbara Costa\*, Eleonora Da Pozzo\*, Chiara Giacomelli, Elisabetta Barresi, Sabrina Taliani, Federico Da Settimo & Claudia Martini

Received: 17 August 2015  
Accepted: 13 November 2015  
Published: 11 January 2016

The pharmacological activation of the cholesterol-binding Translocator Protein (TSPO) leads to an increase of endogenous steroids and neurosteroids determining benefic pleiotropic effects in several pathological conditions, including anxiety disorders. The relatively poor relationship between TSPO ligand binding affinities and steroidogenic efficacies prompted us to investigate the time (Residence Time, RT) that a number of compounds with phenylindolyglyoxylamide structure (PIGAs) spends in contact with the target. Here, given the poor availability of TSPO ligand kinetic parameters, a kinetic radioligand binding assay was set up and validated for RT determination using a theoretical mathematical model successfully applied to other ligand-target systems. TSPO ligand RT was quantified and the obtained results showed a positive correlation between the period for which a drug interacts with TSPO and the compound ability to stimulate steroidogenesis. Specifically, the TSPO ligand RT significantly fitted both with steroidogenic efficacy ( $E_{max}$ ) and with area under the dose-response curve, a parameter combining drug potency and efficacy. A positive relation between RT and anxiolytic activity of three compounds was evidenced. In conclusion, RT could be a relevant parameter to predict the steroidogenic efficacy and the *in vivo* anxiolytic action of new TSPO ligands.

The 18 kDa Translocator Protein (TSPO) is an outer mitochondrial membrane high affinity cholesterol- and drug-binding protein abundant in steroid-producing tissues, including gonads, adrenal, and brain<sup>1</sup>. Previous pharmacological, biochemical and genetic studies, as well as *in vivo* experiments, have provided several lines of evidence demonstrating that TSPO is a key member of the multiprotein complex transducesome, as it participates to the cholesterol translocation into mitochondria, which is considered the rate-limiting step of steroidogenesis<sup>2</sup>.

Consistent with the important role of TSPO in steroidogenesis<sup>3–7</sup> and the involvement of steroids in numerous fundamental processes<sup>8,9</sup>, TSPO ligands have been proposed as innovative therapeutic tools in several pathological conditions. For example, TSPO ligands have been implicated in axonal regeneration<sup>10–12</sup>, in anti-inflammatory<sup>13</sup>, anxiolytic<sup>14–18</sup>, antidepressant<sup>19</sup> and anti-post-traumatic stress<sup>20</sup> activities, both in animal models, and in individuals with neurological or psychiatric disorders. To date, phase II and III clinical trials have been concluded or are ongoing for the treatment of diabetic peripheral neuropathy (ClinicalTrials.gov identifier: NCT00502515), chemotherapy-induced peripheral neuropathy (NCT00868166), and generalized anxiety disorder (NCT00108836).

However, one of the most recurrently issue concerning TSPO ligands consists in the lack of correlation between the binding affinity and the *in vitro* efficacy, including steroidogenic efficacy<sup>21</sup>. This phenomenon has limited not only the identification of lead compounds during the traditional affinity-based drug discovery processes, but also questioned the specificity of the observed effects<sup>22–24</sup>. Recent studies have shown that the affinity of a ligand for its target could not directly define its biological action effectiveness, that it may instead be related to the period for which a drug interacts with its target defined as ‘Residence Time’ (RT)<sup>25,26</sup>.

In the present work, it was investigated whether the RT could be a crucial measure to estimate the steroidogenic efficacy of a TSPO ligand. To this aim, a number of our previous reported TSPO ligands, belonging to phenylindolyglyoxylamides (PIGAs) was selected based on their different abilities to stimulate *in vitro* steroidogenesis<sup>27–29</sup>, Table 1. Among such selected TSPO compounds, three presented *in vivo* anxiolytic effects<sup>28,30,31</sup>.

As a first step, given the poor availability of kinetic parameters for TSPO ligands, a kinetic radioligand binding assay was set up and validated for TSPO ligand RT determination by the use of the theoretical mathematical

Department of Pharmacy, University of Pisa, via Bonanno, 6-56126 Pisa, Italy. \*These authors contributed equally to this work. Correspondence and requests for materials should be addressed to B.C. (email: barbara.costa@farm.unipi.it) or C.M. (email: claudia.martini@unipi.it)

Compd.	R <sub>5</sub>	Ar	R <sub>1</sub>	R <sub>2</sub>
PIGA719 <sup>a</sup>	H	C <sub>6</sub> H <sub>5</sub>	(CH <sub>2</sub> ) <sub>2</sub> CH <sub>3</sub>	(CH <sub>2</sub> ) <sub>2</sub> CH <sub>3</sub>
PIGA720 <sup>a</sup>	H	C <sub>6</sub> H <sub>5</sub>	(CH <sub>2</sub> ) <sub>5</sub> CH <sub>3</sub>	(CH <sub>2</sub> ) <sub>5</sub> CH <sub>3</sub>
PIGA745 <sup>a</sup>	Cl	C <sub>6</sub> H <sub>5</sub>	(CH <sub>2</sub> ) <sub>5</sub> CH <sub>3</sub>	(CH <sub>2</sub> ) <sub>5</sub> CH <sub>3</sub>
PIGA835 <sup>a</sup>	Cl	C <sub>6</sub> H <sub>4</sub> -4-Cl	(CH <sub>2</sub> ) <sub>3</sub> CH <sub>3</sub>	(CH <sub>2</sub> ) <sub>3</sub> CH <sub>3</sub>
PIGA925 <sup>b</sup>	NO <sub>2</sub>	C <sub>6</sub> H <sub>5</sub>	(CH <sub>2</sub> ) <sub>5</sub> CH <sub>3</sub>	(CH <sub>2</sub> ) <sub>5</sub> CH <sub>3</sub>
PIGA1214 <sup>c</sup>	H	C <sub>6</sub> H <sub>4</sub> -4-COOH	(CH <sub>2</sub> ) <sub>5</sub> CH <sub>3</sub>	(CH <sub>2</sub> ) <sub>5</sub> CH <sub>3</sub>
PIGA839 <sup>a</sup>	H	C <sub>6</sub> H <sub>4</sub> -4-CH <sub>3</sub>	(CH <sub>2</sub> ) <sub>2</sub> CH <sub>3</sub>	(CH <sub>2</sub> ) <sub>2</sub> CH <sub>3</sub>
PIGA823 <sup>b</sup>	Cl	C <sub>6</sub> H <sub>4</sub> -4-Cl	CH <sub>2</sub> CH <sub>3</sub>	CH <sub>2</sub> C <sub>6</sub> H <sub>5</sub>
PIGA1128 <sup>c</sup>	H	naphth-2-yl-	(CH <sub>2</sub> ) <sub>2</sub> CH <sub>3</sub>	(CH <sub>2</sub> ) <sub>2</sub> CH <sub>3</sub>
PIGA1138 <sup>c</sup>	H	naphth-2-yl-	CH <sub>3</sub>	(CH <sub>2</sub> ) <sub>4</sub> CH <sub>3</sub>

**Table 1. Structures of PIGAs, PK11195, and Ro5-4864.** <sup>a</sup>Primofiore *et al.*, 2004. <sup>b</sup>DaSettimo *et al.*, 2008. <sup>c</sup>Barresi *et al.*, 2015.

TSPO ligand	Equilibrium K <sub>i</sub> or K <sub>d</sub> (nM)	K <sub>on</sub> (M <sup>-1</sup> , min <sup>-1</sup> )	K <sub>off</sub> (min <sup>-1</sup> )	Kinetically-derived K <sub>d</sub> = K <sub>off</sub> /K <sub>on</sub> (nM)	RT = 1/K <sub>off</sub> (min)
PK11195 (Saturation binding) <sup>a</sup>	3.60 ± 0.41	NA	NA	NA	NA
PK11195 (Displacement) <sup>b</sup>	3.39 ± 0.34	NA	NA	NA	NA
PK11195 (Association and dissociation) <sup>c</sup>		8.30 ± 0.64 × 10 <sup>6</sup>	0.030 ± 0.002	3.61 ± 0.21	33 ± 4
PK11195 (Standard competition association) <sup>d</sup>		9.20 ± 0.71 × 10 <sup>6</sup>	0.034 ± 0.004	3.70 ± 0.43	29 ± 3
PK11195 (Simplified competition assay) <sup>e</sup>		9.30 ± 0.94 × 10 <sup>6</sup>	0.029 ± 0.003	3.12 ± 0.37	34 ± 3
Ro5-4864	20.04 ± 2.36	1.29 ± 0.16 × 10 <sup>6</sup>	0.031 ± 0.002	24.04 ± 2.01	32 ± 3
PIGA719	12.24 ± 1.1	7.89 ± 0.62 × 10 <sup>6</sup>	0.094 ± 0.007	11.95 ± 1.00	11 ± 2
PIGA720	1.40 ± 0.28	2.18 ± 0.29 × 10 <sup>7</sup>	0.039 ± 0.004	1.79 ± 0.24	26 ± 2
PIGA745	13.14 ± 1.16	3.84 ± 0.51 × 10 <sup>6</sup>	0.058 ± 0.003	15.12 ± 1.16	17 ± 1
PIGA823	3.30 ± 0.31	4.30 ± 0.33 × 10 <sup>6</sup>	0.008 ± 0.001	1.86 ± 0.17	127 ± 4
PIGA835	0.91 ± 0.11	5.78 ± 0.56 × 10 <sup>7</sup>	0.058 ± 0.005	1.00 ± 0.19	17 ± 1
PIGA839 (M-PIGA)	5.50 ± 0.47	1.69 ± 0.27 × 10 <sup>6</sup>	0.009 ± 0.001	5.45 ± 0.60	109 ± 4
PIGA925	12.23 ± 3.14	6.78 ± 0.42 × 10 <sup>6</sup>	0.068 ± 0.004	10.01 ± 1.13	15 ± 2
PIGA1128	0.31 ± 0.02	8.10 ± 0.36 × 10 <sup>7</sup>	0.018 ± 0.001	0.22 ± 0.05	55 ± 2
PIGA1138	0.34 ± 0.03	4.30 ± 0.30 × 10 <sup>7</sup>	0.007 ± 0.001	0.17 ± 0.03	141 ± 4
PIGA1214	343.01 ± 15.94	9.05 ± 0.51 × 10 <sup>4</sup>	0.030 ± 0.004	332.05 ± 15.04	39 ± 2

**Table 2. TSPO ligand binding affinity and kinetic parameters obtained by equilibrium binding and kinetic association assays.** Values are means ± SEM of three experiments performed in duplicate. NA = not applicable. <sup>a</sup>[<sup>3</sup>H]PK11195 binding performed using increasing concentration of radioligand. <sup>b</sup>displacement of [<sup>3</sup>H]PK11195 binding using increasing concentration of PK11195. <sup>c</sup>the binding kinetics of [<sup>3</sup>H]PK11195 were determined by 'traditional' association and dissociation assays. <sup>d</sup>the binding kinetics of unlabeled PK11195 were determined by adding a concentration equivalent to one-, three- and ten-fold the K<sub>i</sub> value of PK11195. <sup>e</sup>the binding kinetics of unlabeled PK11195 were determined by adding a concentration equivalent to only three-fold the K<sub>i</sub> value of PK11195.

model of Motulsky and Mahan<sup>32</sup> ( $RT = 1/k_{off}$ , where  $k_{off}$  is the dissociation rate constant). This model has been applied to several ligand-target systems and shown to be highly accurate in determining the binding kinetics of synthetic ligands<sup>33–35</sup>.

## Results

**RT determination: initial setting.** The [<sup>3</sup>H]PK11195 radioligand was used as a probe for the determination of the kinetic parameters using membrane homogenates of rat kidney, a tissue highly rich in TSPO. Initial experiments were performed to fully characterize [<sup>3</sup>H]PK11195 binding kinetic parameters as few literature data were

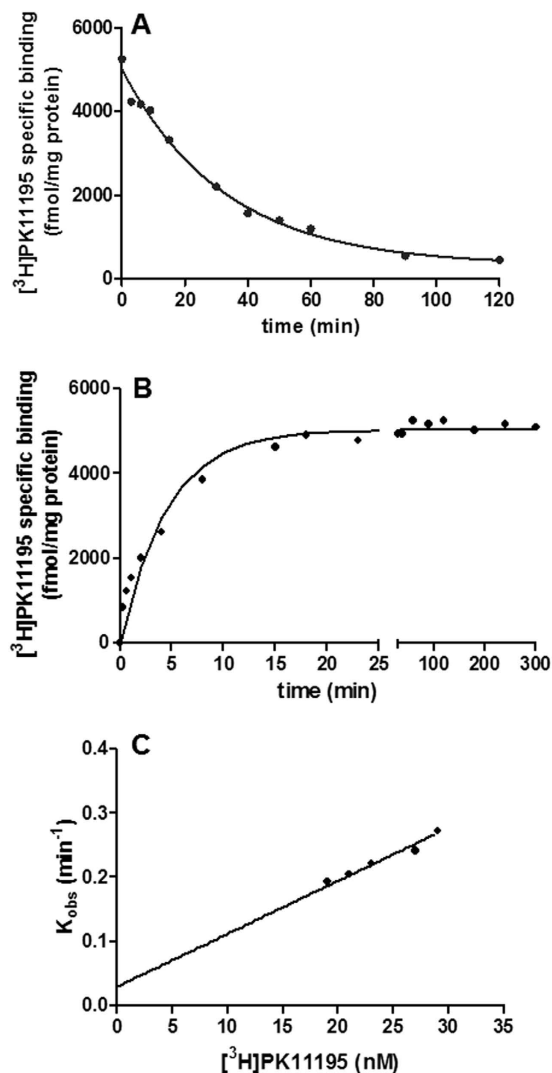


**Figure 1.**  $^3\text{H}]\text{PK11195}$   $k_{\text{on}}$  and  $k_{\text{off}}$  by ‘traditional’ dissociation and association kinetics assays. (A)  $^3\text{H}]\text{PK11195}$  binding dissociation Kinetics: Data were best fitted using a one-phase exponential decay function to produce a  $t_{1/2}$  estimate. This was converted into a  $k_{\text{off}}$  value by using Equation 1, as detailed in the Materials and Methods section. The ordinate reports the specific  $^3\text{H}]\text{PK11195}$  binding expressed as fmol/mg of protein. The abscissa reports the incubation time expressed in min. (B,C)  $^3\text{H}]\text{PK11195}$  binding association Kinetics: a family of association kinetics curves were constructed incubating membrane homogenates with a range of  $^3\text{H}]\text{PK11195}$  concentrations as described in the Materials and Methods section. Data were fitted using a one phase exponential association function to yield a  $k_{\text{obs}}$ . (B) A representative association curve performed using 23 nM  $^3\text{H}]\text{PK11195}$  up to 5 h incubation time is showed. The ordinate reports the specific  $^3\text{H}]\text{PK11195}$  binding expressed as fmol/mg of protein. The abscissa reports the incubation time expressed in min. (C)  $k_{\text{obs}}$  values plotted against the corresponding  $^3\text{H}]\text{PK11195}$  concentration employed are showed.

available<sup>36,37</sup>.  $^3\text{H}]\text{PK11195}$  equilibrium binding parameters,  $K_{\text{d}}$  and  $B_{\text{max}}$ , were  $3.60 \pm 0.41$  nM and  $6498 \pm 500$  fmol/mg of proteins, respectively (Table 2). The  $K_{\text{i}}$  value of unlabeled PK11195 determined by  $^3\text{H}]\text{PK11195}$  displacement binding assay was  $3.39 \pm 0.34$  nM (Table 2).

The  $k_{\text{off}}$  determination was obtained by: (i) pre-labelling of TSPO to equilibrium with one  $^3\text{H}]\text{PK11195}$  concentration (approximately  $10 \times K_{\text{d}}$ ) that provides high initial TSPO occupancy; (ii) inducing radioligand dissociation by addition of TSPO-saturating concentration (about  $1000 \times K_{\text{d}}$ ) of unlabeled competing compound PK11195. Then, the dissociation time-course was analyzed using an exponential function. An example of  $^3\text{H}]\text{PK11195}$  dissociation kinetic curve is shown in Fig. 1A;  $^3\text{H}]\text{PK11195}$  dissociation was monophasic and gave a half-life of radioligand-TSPO complex ( $t_{1/2}$ ) of 23 min, which when applied to Equation 1 (see Materials and Methods section) gave a  $k_{\text{off}}$  of  $0.030 \pm 0.002 \text{ min}^{-1}$ . The RT value, which is the reciprocal of  $k_{\text{off}}$ , was  $33 \pm 4$  min (Table 2).

To determine  $^3\text{H}]\text{PK11195}$   $k_{\text{on}}$ , a family of association kinetic curves using a range of radioligand concentrations were constructed. Each association curve was monitored until equilibrium. In Fig. 1B, a representative  $^3\text{H}]\text{PK11195}$  association kinetics curve is showed. If  $^3\text{H}]\text{PK11195}$  binding follows a simple law of mass action model, the observed kinetic association constant ( $k_{\text{obs}}$ ) should increase in a linear manner with radioligand concentration<sup>38</sup>.

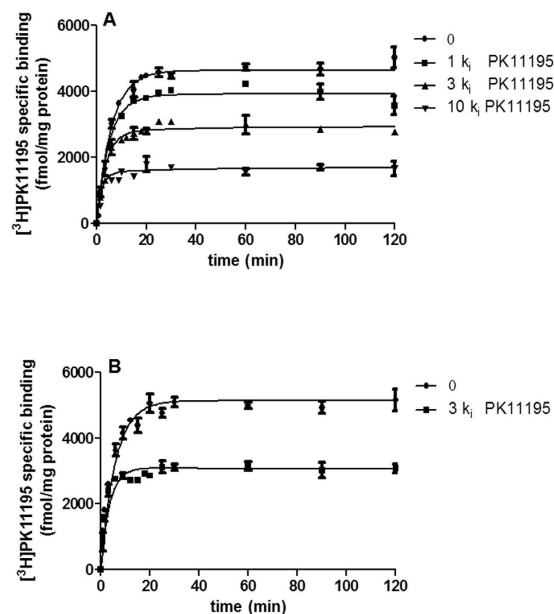


**Figure 2.** PK11195  $k_{\text{on}}$  and  $k_{\text{off}}$  by competitive association kinetics assays. (A) The curves were obtained by incubation of membranes with either radioligand alone or radioligand and unlabeled PK11195 for the indicated time points. Data were fitted to the equation 2 to calculate the  $k_{\text{on}}$  and  $k_{\text{off}}$  of PK11195. Representative curves obtained using one-, three-, ten-fold  $K_i$  value of unlabeled PK11195. (B) Representative curves obtained using three-fold  $K_i$  value of unlabeled PK11195.

In this case, the slope of the line should equate to the association rate and extrapolation of the plot to the Y-intercept (at  $x = 0$ ) should equal the dissociation rate<sup>39</sup>. When the  $k_{\text{ob}}$  values were plotted against radioligand concentration, the data were consistent with a straight line ( $r^2 = 0.98$ ), indicating that binding of  $[^3\text{H}]$ PK11195 to TSPO was consistent with the law of mass action (Fig. 1C). The obtained values were  $k_{\text{on}} = 8.30 \pm 0.64 \times 10^6 \text{ M}^{-1} \text{ min}^{-1}$  and  $k_{\text{off}} = 0.030 \pm 0.002 \text{ min}^{-1}$  (Fig. 1C and Table 2). The kinetically derived  $K_d$  ( $3.61 \pm 0.21 \text{ nM}$ ; kinetic  $K_d = k_{\text{off}}/k_{\text{on}}$ ) was in good agreement with the value obtained from  $[^3\text{H}]$ PK11195 saturation experiments (equilibrium  $K_d = 3.60 \pm 0.41$ ) (Table 2).

**RT Determination: TSPO ligand  $k_{\text{off}}$  and  $k_{\text{on}}$  by competition kinetic association assays.** With the predetermined  $k_{\text{on}}$  ( $k_1$ ) and  $k_{\text{off}}$  ( $k_2$ ) values of  $[^3\text{H}]$ PK11195 from ‘traditional’ kinetic association and dissociation experiments,  $k_{\text{on}}$  ( $k_3$ ) and  $k_{\text{off}}$  ( $k_4$ ) of an unlabeled ligand could be determined by fitting the kinetic parameters into the model of ‘Kinetics of competitive binding’ described in Materials and Methods section. This method is based on a framework developed by Motulsky and Mahan<sup>32</sup>, where an unlabeled competitor is added simultaneously with a radioligand to the receptor preparation of interest. Then, the experimentally derived rate of specific radioligand binding can be modelled to provide the association and dissociation rates of the unlabeled compound.

As a first step, the competition association assay was performed using unlabeled PK11195. Three different concentrations of PK11195 were tested to ensure that the rate parameters calculated were independent of ligand concentration (Fig. 2A). The  $k_{\text{on}}$  ( $k_3$ ) and  $k_{\text{off}}$  ( $k_4$ ) values determined in this assay were  $9.20 \pm 0.71 \times 10^6 \text{ M}^{-1} \text{ min}^{-1}$  and  $0.034 \pm 0.004 \text{ min}^{-1}$ , respectively (Table 2; PK11195 RT =  $29 \pm 3 \text{ min}$ ), which corresponded rather well to the kinetics rates determined by ‘traditional’ association and dissociation experiments (Table 2). Moreover, the kinetically derived  $K_d$  obtained from the competition association assay for unlabeled PK11195 was similar to  $K_i$  obtained from displacement experiments and  $K_d$  derived from saturation experiments (Table 2). Taken together, these findings proved that the competition association assay could be applied to determine the binding kinetics of an unlabeled TSPO ligand.

The competition association assay approach has been shown to be highly accurate in determining the binding kinetics at several targets<sup>33–35</sup>. However, when the kinetics of multiple compounds need to be determined, the standard model is laborious and time consuming because it implies the use of three concentrations of each unlabeled ligand. Recently, it has been demonstrated that the use of one concentration of unlabeled ligand is able to yield an accurate determination of kinetic rates of unlabeled ligands at their receptor, too<sup>34</sup>. These findings prompted us to modify the three-concentration-dependent assay into a one-concentration-based method. The data analyzed at three-fold  $K_i$  of unlabeled PK11195 showed a comparable result ( $k_{\text{on}} = 9.30 \pm 0.94 \times 10^6 \text{ M}^{-1} \text{ min}^{-1}$  and  $k_{\text{off}} = 0.029 \pm 0.003 \text{ min}^{-1}$ ; RT =  $34 \pm 3 \text{ min}$ ) (Fig. 2B) to that generated in a standard (three-concentration-dependent) competition association experiment (Table 2). This result indicates that this simplified method is strong enough to quantify the binding kinetics, which eventually enables testing in a faster medium-throughput format, yet without loss of accuracy.

By using the ‘simplified’ competition kinetic association assay, the TSPO ligands, including the classical ones Ro5-4864 and PIGA compounds (Table 1) were tested at three-fold respective  $K_i$  concentration and data were

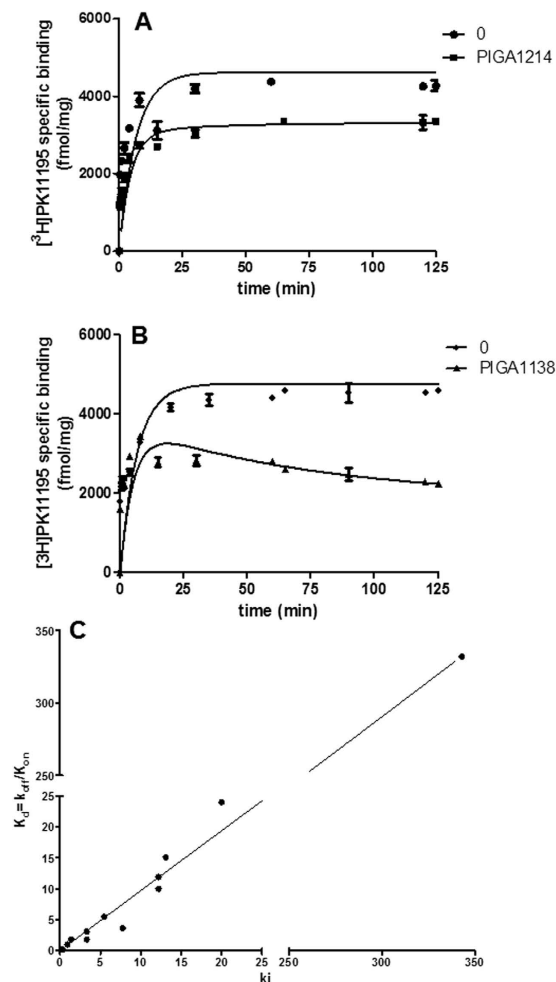


**Figure 3. Competitive association kinetics assays of TSPO ligands and correlation between  $K_i$  and ‘Kinetic  $K_d$ ’ values.** (A) Representative curves obtained using three-fold  $K_i$  of PIGA1214 (B) or PIGA1138. (C)  $K_i$  values were obtained from  $[^3\text{H}]$ PK11195 competition binding experiments at equilibrium. The kinetically  $K_d$  values were derived from the competition association experiments.

fitted using Equation 2 (see Material and Methods section) to calculate  $k_{\text{on}}$  and  $k_{\text{off}}$  simultaneously (Table 2). Competition association assay results demonstrated two patterns of  $[^3\text{H}]$ PK11195 binding in dependence of the competing ligand used. In general, if the competitor dissociates from its target faster than the radioligand, the specific binding of the radioligand will approach its equilibrium time slowly and monotonically. However, when the competitor dissociates slower, the association curve of the radioligand will consist of two phases, starting with a typical “overshoot” and then a decline until a new equilibrium is reached. The results obtained are consistent with a rapid (PIGA719, PIGA720, PIGA745, PIGA835, PIGA925, PIGA1214, Ro5-4864) and a slow (PIGA823, PIGA839 (M-PIGA), PIGA1128, PIGA1138) dissociation rate of the ligands from TSPO. Representative curves for rapid dissociating (PIGA1214) and slow dissociating (PIGA1138) TSPO ligands were shown in Fig. 3A,B, respectively.

To validate the rate constants, the kinetically derived  $K_d$  were compared with  $K_i$  obtained from equilibrium competition binding experiments. Notably, an excellent correlation ( $r^2 = 0.999$ ,  $p < 0.0001$ ; Fig. 3C) was observed between  $K_i$  determined in equilibrium-binding studies and  $K_d$  values derived from the competition association assays (Table 2). This further proved that the simplified model is able to quantify the association and dissociation rates of unlabeled TSPO ligands accurately.

**TSPO ligand steroidogenic efficacy.** The steroidogenic efficacy of TSPO ligands was measured in terms of pregnenolone production in C6 glioma cells following exposure with increasing ligand concentrations for a fixed incubation time. For each TSPO ligand, potency ( $EC_{50}$  value) was derived by sigmoidal concentration-dependent curve and efficacy ( $E_{\text{max}}$  value, relative to the highest tested concentration of TSPO ligand) was calculated with respect to control (DMSO-treated sample), corresponding to basal pregnenolone production. In Fig. 4, the curves of TSPO ligand-stimulated pregnenolone production are shown. The  $EC_{50}$  and  $E_{\text{max}}$  values are detailed in Table 3. Specifically, among all tested TSPO ligands, M-PIGA, PIGA823 and PIGA1138 had the highest efficacy. The majority of the tested TSPO ligands showed efficacy to stimulate pregnenolone production ranging from 140% up to 179% (basal value was set to 100%).

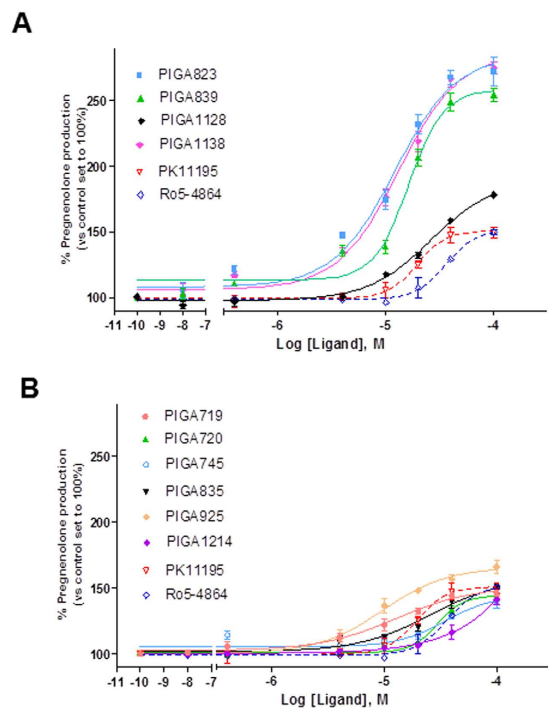


**Figure 4.** Effects of the TSPO ligands (PK11195, Ro4-54864, PIGAs) on glioma C6 cell steroid synthesis. (A) Dose-dependent effects of the compounds with longest RTs (>40 min) on C6 steroidogenesis (B) Dose-dependent effects of the compounds with shortest RTs (<40 min) on C6 steroidogenesis. C6 cells were cultured with increasing concentrations of ligands (0–100 μM) for 2 h in serum-free media and pregnenolone released into the media was assessed by ELISA. The results are expressed as the mean of three separate experiments, and data were fitted with a dose–response curve with Hill slope of 1.0.

TSPO ligand	EC <sub>50</sub> (μM)	E <sub>max</sub> (at 100 μM) (vehicle set to 100%)	Equilibrium K <sub>i</sub> or K <sub>d</sub> (nM)	RT (min)
PK11195	19.5 ± 1.8	153 ± 4	3.30 ± 0.34	34 ± 3
Ro5-4864	36.2 ± 2.5	150 ± 4	20.04 ± 2.36	32 ± 3
PIGA719	12.9 ± 1.5	146 ± 2	12.24 ± 1.1	11 ± 2
PIGA720	29.7 ± 3.1	144 ± 4	1.40 ± 0.28	26 ± 2
PIGA745	34.6 ± 3.6	140 ± 5	13.14 ± 1.16	17 ± 1
PIGA823	12.2 ± 1.3	272 ± 11	3.30 ± 0.31	127 ± 4
PIGA835	25.6 ± 2.3	149 ± 4	0.91 ± 0.11	17 ± 1
PIGA839 (M-PIGA)	16.3 ± 1.4	254 ± 5	5.50 ± 0.47	109 ± 4
PIGA925	9.71 ± 1.0	166 ± 5	12.23 ± 3.14	15 ± 2
PIGA1128	26.1 ± 1.5	179 ± 7	0.31 ± 0.02	55 ± 2
PIGA1138	13.1 ± 1.4	275 ± 5	0.34 ± 0.03	141 ± 4
PIGA1214	92.0 ± 5.6	141 ± 4	343.01 ± 15.94	39 ± 2

**Table 3.** Experimental kinetic/thermodynamic data and steroidogenic parameters for TSPO ligands. Values are means ± SEM of three experiments performed in duplicate. Potency (EC<sub>50</sub> value) of TSPO ligands was derived by sigmoidal concentration-dependent curves. Efficacy (E<sub>max</sub>) corresponds to amount of pregnenolone production by 100 μM TSPO ligand concentration.

**Correlation between RT and steroidogenesis efficacy.** In Fig. 5, correlation analyses are reported between the TSPO ligand-mediated steroidogenic potency or efficacy and either binding affinity (K<sub>i</sub>) or Residence Time (RT). The steroidogenic potency of TSPO ligands correlated with the logarithm of K<sub>i</sub> (Pearson  $r = 0.6553$ ;  $P = 0.0207$ ;  $r^2 = 0.4295$ ) (Fig. 5A), in agreement with previous reported data<sup>40–42</sup>, but not with RT (Pearson  $r = 0.08962$ ;  $P = 0.7818$ ;  $r^2 = 0.0803$ ) (Fig. 5B). The steroidogenic efficacy of TSPO ligands did not significantly correlate with K<sub>i</sub> (Pearson  $r = -0.3489$ ;  $P = 0.2663$ ;  $r^2 = 0.1217$ ) (Fig. 5C). Conversely, a highly significant correlation was observed between steroidogenic efficacy and RT (Pearson  $r = 0.8526$ ;  $P = 0.0004$ ;  $r^2 = 0.7270$ ) (Fig. 5D). Correlation analyses were also performed between the logarithm of K<sub>i</sub> or RT and the area under the dose–response curve (AUC), a value that combines potency and efficacy of a drug into a single parameter<sup>43</sup>. When the relationship

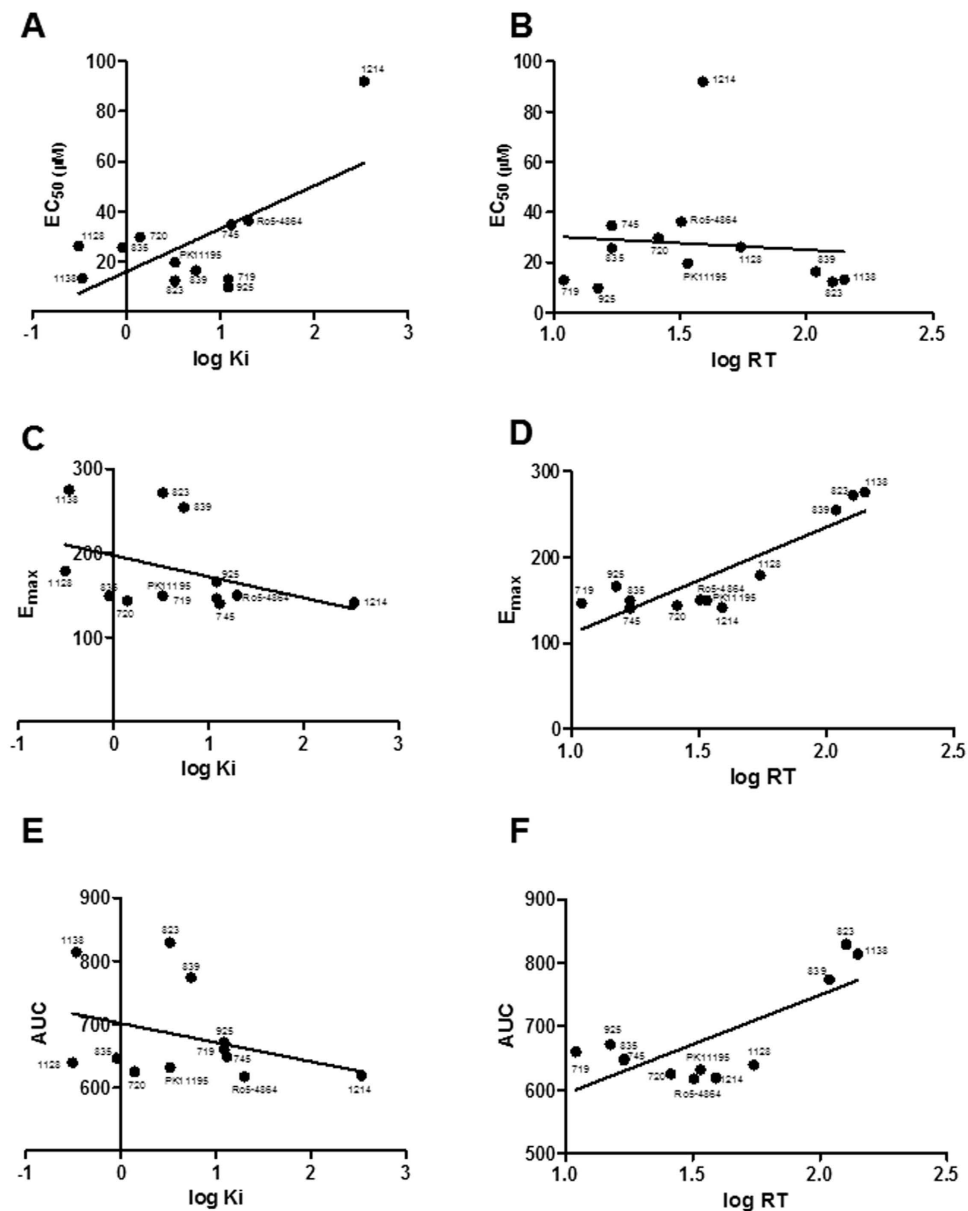


**Figure 5. Correlation analyses between kinetic/thermodynamic and steroidogenic parameters.** TSPO compound names were included next to their respective data points (for PIGA compounds only the ID numbers were shown). (A) Scatter plot of the  $EC_{50}$  values against thermodynamic parameters ( $\log K_i$ ) of test TSPO ligands; (B) Scatter plot of the  $EC_{50}$  values against kinetic parameters ( $\log RT$ ) of test TSPO ligands; (C) Scatter plot of the  $E_{\max}$  values against thermodynamic parameters ( $\log K_i$ ) of test TSPO ligands; (D) Scatter plot of the  $E_{\max}$  values against kinetic parameters ( $\log RT$ ) of test TSPO ligands; (E) Scatter plot of the AUC values against thermodynamic parameters ( $\log K_i$ ) of test TSPO ligands; (F) Scatter plot of the AUC values against kinetic parameters ( $\log RT$ ) of test TSPO ligands.

between AUC and the logarithm of  $K_i$  was analyzed, no correlation was found (Pearson  $r = -0.3308$ ;  $P = 0.2937$ ;  $r^2 = 0.1094$ ) (Fig. 5E). On the contrary, the AUC values significantly correlates with logarithm of RT (Pearson  $r = 0.7563$ ;  $P = 0.0044$ ;  $r^2 = 0.5720$ ) (Fig. 5F).

## Discussion

The TSPO drug discovery has followed the traditional thermodynamic equilibrium constant ( $K_d$  or  $K_i$ ) paradigm to identify lead compounds. However, binding kinetics parameters, especially the Residence Time of a drug on its target, are becoming critical predictors for *in vivo* drug efficacy<sup>25,26</sup>. In the present manuscript, accurate kinetic parameters for TSPO ligands were obtained by the use of the mathematical model of Motulsky and Mahan<sup>32</sup> that has been shown to be highly accurate in determining the binding kinetics of unlabeled ligands at several targets<sup>33–35</sup>. This mathematical model has overcome the high cost of compound radiolabeling in order to measure directly the association and dissociation rates of a drug to the target<sup>44</sup>. For binding kinetics determination, classical TSPO

ligands (the isoquinoline PK11195 and the benzodiazepine Ro5-4864) and the TSPO ligand PIGAs<sup>27–29</sup> (Table 1) were selected. Specifically, the majority of the tested TSPO compounds resulted rapid dissociating competitors of [<sup>3</sup>H]PK11195 binding sites (PIGA719, PIGA720, PIGA745, PIGA835, PIGA925, PIGA1124 and Ro5-4864) (Table 2). Conversely, the compound PIGA823, PIGA839 (M-PIGA), PIGA1128, and PIGA1138 resulted slow dissociating competitors (Table 2). Concerning the molecular determinants underlying the TSPO-ligand kinetic interactions, no literature data are available. The estimation of the RT for a large number of TSPO ligands could support in determining new Structure Activity Relationship (SAR) based on the ligand kinetic parameters. Indeed up to date, SAR has been rationalized only on binding affinity parameters using pharmacophore hypotheses<sup>27,28,45,46</sup> and a 3D model<sup>29</sup> based on the newly published NMR structure of mouse TSPO (PDB code 2MGY)<sup>47</sup>. Notably, the steroidogenic efficacy of TSPO ligands did not correlated with the compound binding affinity<sup>21</sup>, suggesting the limitation of a SAR affinity-based strategy.

Herein, a highly significant positive correlation between the efficacy to stimulate *in vitro* steroidogenesis of TSPO ligands and their kinetic parameter RT was found. Remarkably, the efficacy did not correlate with the thermodynamic equilibrium constant  $K_i$  of the TSPO ligands. Taken together, these results indicate that the key factor for robust steroidogenic TSPO ligand efficacy is not the binding affinity *per se*, but rather the time the compound spends on the target. Such this novel concept for TSPO ligands suggests the importance of using the RT parameter rather than the constant  $K_i$  during the *in vitro* characterization of TSPO compounds in relation to their steroidogenic activity.

The results discussed thus far allow us to outline a preliminary efficacy-based SAR for the interaction of PIGAs with TSPO. Data in Table 2 suggest a cooperative effect between the size of the substituents on the amide nitrogen and the lipophilicity of the aryl group at the 2-indole position. In particular, high retention times and high efficacy seem to derive from the presence of an highly lipophilic moiety at the 2-position ( $C_6H_4-4-CH_3$ ,  $C_6H_4-4-Cl$ , naphth-2-yl), combined with at least one of the two *N*-alkyl groups with a number of carbon atoms in the 1–3 range (PIGA839, PIGA823, PIGA1138).

From a therapeutic perspective, this new concept paves the way to identify TSPO drugs with promising pharmacological activities, including anxiolytic effects. Scientific community has directed particular interest to TSPO ligands for the treatment of anxiety-related disorders, as they have shown fast-acting anxiolytic properties without the typical side-effects of benzodiazepine-based regimes<sup>15,48,49</sup>. Differently to benzodiazepines, which act as direct modulators of the GABA<sub>A</sub> receptor, TSPO ligands generally enhance GABAergic neurotransmission via the promotion of neurosteroidogenesis without direct effects at the GABA<sub>A</sub> receptor<sup>17</sup>. Neurosteroids, especially the 3- $\alpha$ -reduced steroids, are potent positive allosteric modulators of GABA<sub>A</sub> receptor<sup>17</sup>. Consistent with such evidences, previous our data<sup>30</sup> have shown that the medium from PIGA839 (M-PIGA)-treated human glial cell model contained high levels of allopregnanolone, one of the major positive GABA<sub>A</sub> receptor allosteric modulator. The conditioned medium potentiated the <sup>36</sup>Cl<sup>-</sup> uptake into cerebral cortical synaptoneuroosomes, suggesting a positive modulation of GABA<sub>A</sub> receptor activity<sup>30</sup>. The PIGA ligands have been already tested for their potential *in vivo* anxiolytic effects by means of the Elevated Plus-Maze (EPM) paradigm in the rat (PIGA823: compound number 32 in<sup>28</sup>, and PIGA839 (M-PIGA) in<sup>30</sup>). In the EPM test, either PIGA823 and PIGA839 (M-PIGA), characterized by long RT and high steroidogenic efficacy, have elicited a significant anxiolytic activity (PIGA823: RT = 127 min,  $E_{max}$  pregnenolone = 272%; PIGA839 (M-PIGA): RT = 109 min;  $E_{max}$  pregnenolone = 254%). Conversely, it has been documented that the classical TSPO ligand PK11195 and Ro5-4864, which are characterized by shorter RT and lower pregnenolone  $E_{max}$  (PK11195: RT = 34 min,  $E_{max}$  pregnenolone = 153%; Ro5-4864: RT = 32 min;  $E_{max}$  pregnenolone = 150%) than PIGA823 and PIGA839 (M-PIGA), does not determine anxiolytic effect in EPM test<sup>50</sup>. In addition, PK11195 has been used to antagonize anxiolytic effects exerted by other TSPO ligands (high steroidogenic efficacy, such as FGIN-1-27, FGIN-1-44 and YL-IPA08)<sup>4,6,19</sup>. These retrospective assessments suggested that a long RT predicts the anxiolytic activity of a TSPO ligand. Moreover, RT is a better efficacy predictive measure than the thermodynamic equilibrium constant  $K_d$  or  $K_i$ . Indeed, PK11195, PIGA823 and PIGA839 (M-PIGA) showed comparable  $K_i$  values (PK11195:  $K_i$  = 3.60 nM; PIGA823  $K_i$  = 3.30 nM; PIGA839 (M-PIGA)  $K_i$  = 5.50 nM), irrespective to their *in vivo* activity. Consistent with our data, it has been recently demonstrated discrepancy between the  $K_i$  of known anxiolytic TSPO ligands (Etifoxine and XBD173) and the enhancement of neurosteroid synthesis<sup>21</sup>. Specifically, Etifoxine, which is already clinically approved for the treatment of anxiety-related disorders, is more potent to stimulate neurosteroidogenesis than XBD173, although its binding affinity to TSPO was approximately 140 fold lower than XBD173. These findings have suggested that the efficacy of such TSPO ligands to stimulate neurosteroid synthesis, thereby leading to anxiolytic effects, cannot be concluded from their binding affinity to TSPO.

In conclusion, the present results indicate that the Residence Time is a better parameter to estimate the steroidogenic effectiveness of a TSPO ligand compared to the equilibrium thermodynamic parameters, corroborating the importance of the drug-target interaction dynamics in predicting the drug efficacy. These findings, in combination with the future availability of a RT database, open the way to optimize TSPO ligands as promising therapeutic tools.

## Materials and Methods

**Reagents.** [<sup>3</sup>H]PK11195 (Specific Activity, 85.7  $\mu$ Ci/nmol) and Ultima Gold scintillation mixture were obtained from Perkin-Elmer Life Sciences. PK11195, protease inhibitors and GF/C glass fiber filters were purchased from Sigma-Aldrich. 2-arylindol-3-ylglyoxyl derivatives were synthesized as previously described<sup>27–29</sup>. Dulbecco's modified Eagle's medium, fetal bovine serum, L-glutamine, penicillin, and streptomycin were from Lonza (Milano, Italy). Enzyme immunoassay (ELISA) for pregnenolone measurement was obtained from IBL (Hamburg, Germany). SU10603 and trilostane were gifts from Novartis Farma (Varese, Italy) and Dr. Zister (University of Dublin, Dublin, Ireland), respectively. Protein assay reagent was obtained by Bio-Rad Laboratories Inc. All other chemical reagents were obtained by commercial sources.



**[<sup>3</sup>H]PK11195 binding saturation assays.** Membranes from rat kidneys were prepared as described previously<sup>51</sup>. All the experimental procedures were carried out following the guidelines of the European Community Council Directive 86–609 and have been approved by the Committee for animal experimentation of the University of Pisa. The resulting membrane pellets were aliquoted and frozen at –20 °C. For all radioligand binding assays, an aliquot of membranes was thawed, suspended in assay buffer (AB, Tris-HCl 50 mM, pH 7.4) and homogenized using Ultraturrax. In cell membrane homogenate, protein content was measured by the Bradford method<sup>52</sup> using the Bio-Rad Protein Assay reagent.

Membrane homogenates (30 μg of proteins) were incubated with increasing [<sup>3</sup>H]PK11195 concentrations (0.1–20 nM; Specific Activity, 85.7 μCi/nmol) in the final volume of 500 μl of AB for 90 min at 0 °C. Non-specific [<sup>3</sup>H]PK11195 binding was obtained in the presence of 1 μM PK11195 (solubilized with ethanol); the solvent concentration was less than 1% and did not interfere with specific [<sup>3</sup>H]PK11195 binding. After incubation time, samples were filtered rapidly under vacuum through GF/C glass fiber filters. After being washed three times with 3 ml of AB, radioactivity trapped on the filter was measured by liquid scintillation counter (TopCount; PerkinElmer Life and Analytical Sciences; 65% counting efficiency).

**PIGA TSPO ligands.** The compounds PIGA719, PIGA720, PIGA745, PIGA835, PIGA839 (M-PIGA)<sup>27</sup>, PIGA925, PIGA823, PIGA922<sup>28</sup>, PIGA1214, PIGA1128, PIGA1138 were synthesized following experimental procedure previously described by us<sup>29</sup>.

**[<sup>3</sup>H]PK11195 binding displacement assays.** Membrane homogenates (20 μg of proteins) were incubated with increasing concentrations of unlabeled TSPO ligand and 1 nM [<sup>3</sup>H]PK11195 (Specific Activity, 85.7 μCi/nmol) in the same above described conditions. The inhibitory constant ( $K_i$ ) determination was performed for PK11195 and additional compounds, including Ro5-4864 (Sigma-Aldrich Milano, Italy) and PIGA ligands<sup>27–29</sup>.

**[<sup>3</sup>H]PK11195 binding 'traditional' kinetics assays.** The [<sup>3</sup>H]PK11195  $k_{off}$  was determined by incubating membrane homogenates (30 μg of protein) with [<sup>3</sup>H]PK11195 at one fixed concentration, corresponding to approximately ten-fold its  $K_d$  value, in a final volume of 500 μl AB at 0 °C. To obtain [<sup>3</sup>H]PK11195 concentration, corresponding to  $10 \times K_d$ , approximately 1.5 μCi of [<sup>3</sup>H] had to be added per assay. Since 1 μCi of [<sup>3</sup>H] per assay represents the practical upper limit of radiotracer usage, the radioligand was diluted with unlabeled PK11195 to reduce its specific activity. In brief, the specific activity of [<sup>3</sup>H]PK11195 was reduced to ¼ of its initial original specific activity (Specific Activity, 21.4 μCi/nmol). This allowed us to use a maximum amount of approximately 0.38 μCi of [<sup>3</sup>H] per sample. After a pre-incubation of 2 h, the dissociation was initiated by addition of 5 μM PK11195. The amount of radioligand bound to TSPO was measured at various time intervals for a total duration of 2 h.

To determine [<sup>3</sup>H]PK11195  $k_{on}$ , the observed association rate constant ( $k_{ob}$ ) was calculated at different concentrations of [<sup>3</sup>H]PK11195 (Specific Activity, 21.4 μCi/nmol). The experiment was initiated ( $t = 0$ ) by addition of [<sup>3</sup>H]PK11195 to membrane homogenates (30 μg of proteins) in a final volume of 500 μl of AB and incubated up to 2 h. To establish whether [<sup>3</sup>H]PK11195 binding was stable for longer times than 2 h, incubation times were prolonged up to 5 h in some kinetic association binding assays. Free [<sup>3</sup>H]PK11195 was separated at multiple time points to construct association kinetic curves. Incubations for both the [<sup>3</sup>H]PK11195 dissociation and association assays were terminated and samples were obtained as above described.

**Unlabeled TSPO ligand competition kinetic association assays.** The unlabeled TSPO ligand kinetic parameters were assessed using the theoretical model of Motulsky and Mahan<sup>32</sup>. Unlike methods in which one compound is pre-equilibrated with the receptor, this approach involves the simultaneous addition of both radioligand and competitor to receptor preparation, so that at  $t = 0$  all receptors are unoccupied. [<sup>3</sup>H]PK11195 (approximately 30 nM; SA, 21.4 μCi/nmol) was added simultaneously with unlabeled compound to membrane homogenates (30 μg of proteins) in a final volume of 500 μl AB. The degree of bound to TSPO was assessed at multiple time points by filtration harvesting and liquid scintillation counting, as above described. The assay was performed using concentration of PK11195 corresponding to one-, three- and ten-fold its  $K_i$ . For 'simplified' competition kinetic association assays, the experiments were performed using concentration of unlabeled TSPO ligands corresponding to three-fold their  $K_i$ .

**Pregnenolone measurement.** Pregnenolone assessment was performed using rat C6 glioma cells as an *in vitro* steroidogenic model, as previously described<sup>29</sup>. C6 cells were cultured in Dulbecco's modified Eagle's medium supplemented with 10% fetal bovine serum, 2 M L-glutamine, penicillin at 100 U/mL, and streptomycin at 100 μg/mL. Cell cultures were maintained in a humidified atmosphere of 5% CO<sub>2</sub> and 95% air at 37 °C. Before the measurement of pregnenolone production, the cells (seeded in 96-well plates at a density of  $\sim 10^5$  cells/well) were washed 2 times with a salt medium, consisting of 140 mM NaCl, 5 mM KCl, 1.8 mM CaCl<sub>2</sub>, 1 mM MgSO<sub>4</sub>, 10 mM glucose, and 10 mM N-2-hydroxyethylpiperazine-N'-2-ethanesulfonic acid (HEPES)–NaOH (pH 7.4) plus 0.1% bovine serum albumin. For the measurement of pregnenolone secreted into the medium, the further metabolism of pregnenolone was blocked by the addition of trilostane (25 μM) and SU10603 (10 μM) (inhibitors of 3β-hydroxysteroid dehydrogenase and 17α-hydroxylase, respectively) to the salt medium. The addition of PK11195, Ro5-4864 or PIGAs to the C6 cells was accomplished by complete change of the salt medium to a medium containing increasing concentrations of the compounds (ranging from 0 to 100 μM). The final concentration of vehicle (DMSO or ethanol) was constant for all of the samples and did not exceed 0.5% (v/v), a concentration that did not affect steroid production on its own. At the end of the incubation periods (2 hours), the cell medium was collected and the amount of pregnenolone secreted into the medium was quantified by an enzyme immunoassay, under the conditions recommended by the supplier. Cross-reactivity with other steroids was typically less than 1%

and cross-reactivity with progesterone is 6%. The sensitivity of the assay was 0.05 ng/ml. Unknown samples were compared with concurrently run standards of pregnenolone using a one-site competition model (calibrator curve).

**Data analysis.** All experiments were analyzed by either linear or non linear regression using Prism 5.0 (GraphPad Software Inc., San Diego, CA). Equilibrium  $K_d$  and maximum binding sites ( $B_{max}$ ) values of [ $^3H$ ]PK11195 at TSPO were obtained by computational analysis of saturation curves. Competition displacement binding were fitted to sigmoidal (variable slope) curves. The concentration of test compounds that inhibited [ $^3H$ ]PK11195 binding to kidney membranes by 50% ( $IC_{50}$  values) obtained from the inhibition curves were converted to  $K_i$  values using the method of Cheng and Prusoff<sup>33</sup>. [ $^3H$ ]PK11195 dissociation data were fitted to a one-phase exponential decay function and the  $t_{1/2}$  value obtained was transformed into a  $k_{off}$  rate using the Equation:

$$k_{off} = \frac{\ln 2}{t_{1/2}} \quad (1)$$

[ $^3H$ ]PK11195 association data were fitted to a single phase exponential association function to calculate an observed rate constant  $k_{ob}$ .

Association and dissociation rates for unlabeled TSPO ligands were calculated by fitting the data in the competition association model using the 'kinetics of competitive binding' assay, defining the amount of radioligand bound to receptor ([RL]) as a function of time<sup>32</sup>:

$$[RL] = \frac{Nk_1[L]}{K_F - K_S} \left[ \frac{k_4(K_F - K_S)}{K_F K_S} + \frac{(k_4 - K_F)}{K_F} \exp(-K_F t) - \frac{(k_4 - K_S)}{K_S} \exp(-K_S t) \right] \quad (2)$$

$$K_F = 0.5 [(K_A + K_B + \sqrt{(K_A - K_B)^2 + 4k_1k_3[L][I]})]$$

$$K_S = 0.5 [(K_A + K_B + \sqrt{(K_A - K_B)^2 + 4k_1k_3[L][I]})]$$

$$K_A = k_1 [L] + k_2$$

$$K_B = k_3 [I] + k_4$$

The abbreviations used are: [RL] is the receptor-radioligand complex, as the specific [ $^3H$ ]PK11195 binding (fmol/mg of protein); [L] is the concentration of [ $^3H$ ]PK11195 used (nM), [I] is the concentration of unlabeled ligand (nM); t is the time in min; N is the total concentration of TSPO (fmol/mg of protein);  $k_1$  and  $k_2$  are the  $k_{on}$  ( $M^{-1} \text{min}^{-1}$ ) and  $k_{off}$  ( $\text{min}^{-1}$ ) of [ $^3H$ ]PK11195, respectively, determined from the radioligand association assay;  $k_3$  is the  $k_{on}$  value ( $M^{-1} \text{min}^{-1}$ ) of the unlabeled ligand;  $k_4$  is the  $k_{off}$  value ( $\text{min}^{-1}$ ) of the unlabeled ligand.

Correlation analyses were performed by Pearson correlation.

## References

- Batarseh, A. & Papadopoulos, V. Regulation of translocator protein 18 kDa (TSPO) expression in health and disease states. *Mol. Cell. Endocrinol.* **327**, 1–12 (2010).
- Papadopoulos, V. *et al.* Translocator protein-mediated pharmacology of cholesterol transport and steroidogenesis. *Mol. Cell. Endocrinol.* **408**, 90–98 (2015).
- Korneyev, A. *et al.* Stimulation of brain pregnenolone synthesis by mitochondrial diazepam binding inhibitor receptor ligands *in vivo*. *J. Neurochem.* **61**, 1515–1524 (1993).
- Romeo, E. *et al.* Stimulation of brain steroidogenesis by 2-aryl-indole-3-acetamide derivatives acting at the mitochondrial diazepam-binding inhibitor receptor complex. *J. Pharmacol. Exp. Ther.* **267**, 462–471 (1993).
- Serra M. *et al.* 2-Phenyl-imidazo[1,2-a]pyridine derivatives as ligands for peripheral benzodiazepine receptors: stimulation of neurosteroid synthesis and anticonflict action in rats. *Br. J. Pharmacol.* **127**, 177–187 (1999).
- Bitran, D., Foley, M., Audette, D., Leslie, N. & Frye, C. A. Activation of peripheral mitochondrial benzodiazepine receptors in the hippocampus stimulates allopregnanolone synthesis and produces anxiolytic-like effects in the rat. *Psychopharmacology.* **151**, 64–71 (2000).
- Verleye, M. The anxiolytic etifoxine activates the peripheral benzodiazepine receptor and increases the neurosteroid levels in rat brain. *Pharmacol. Biochem. Behav.* **82**, 712–720 (2005).
- Yuki, A. *et al.* Relationship between low free testosterone levels and loss of muscle mass. *Sci. Rep.* **3**, 1818 (2013).
- Ankrum, J. A., Dastidar, R. G., Ong, J. E., Levy, O. & Karp, J. M. Performance-enhanced mesenchymal stem cells via intracellular delivery of steroids. *Sci. Rep.* **4**, 4645 (2014).
- Ferzaz, B. *et al.* SSR180575 (7-chloro-N,N,5-trimethyl-4-oxo-3-phenyl-3,5-dihydro-4H-pyridazo[4,5-b]indole-1-acetamide), a peripheral benzodiazepine receptor ligand, promotes neuronal survival and repair. *J. Pharmacol. Exp. Ther.* **301**, 1067–1078 (2002).
- Girard, C. *et al.* Etifoxine improves peripheral nerve regeneration and functional recovery. *Proc. Natl. Acad. Sci. USA* **105**, 20505–20510 (2008).
- Girard, C. Axonal regeneration and neuroinflammation: roles for the translocator protein 18 kDa. *Neuroendocrinol.* **24**, 71–81 (2012).
- Torres, S. R. Anti-inflammatory effects of peripheral benzodiazepine receptor ligands in two mouse models of inflammation. *Eur. J. Pharmacol.* **408**, 199–211 (2000).
- Bitran, D., Foley, M., Audette, D., Leslie, N. & Frye, C. A. Activation of peripheral mitochondrial benzodiazepine receptors in the hippocampus stimulates allopregnanolone synthesis and produces anxiolytic-like effects in the rat. *Psychopharmacology.* **151**, 64–71 (2000).
- Kita, A. *et al.* Antianxiety and antidepressant-like effects of AC-5216, a novel mitochondrial benzodiazepine receptor ligand. *Br. J. Pharmacol.* **142**, 1059–1072 (2004).
- Rupprecht, R. *et al.* Translocator protein (18 kDa) (TSPO) as a therapeutic target for neurological and psychiatric disorders. *Nat. Rev. Drug. Discov.* **9**, 971–988 (2010).

17. Da Pozzo, E., Costa, B. & Martini, C. Translocator protein (TSPO) and neurosteroids: implications in psychiatric disorders. *Curr. Mol. Med.* **12**, 426–442 (2012).
18. Costa, B., Da Pozzo, E. & Martini, C. Translocator protein as a promising target for novel anxiolytics. *Curr. Top. Med. Chem.* **12**, 270–285 (2012).
19. Zhang, L. M. *et al.* Antidepressant-like and anxiolytic-like effects of YL-IPA08, a potent ligand for the translocator protein (18 kDa). *Neuropharmacology* **81**, 116–125 (2014).
20. Zhang, L. M. *et al.* Anxiolytic-like effects of YL-IPA08, a potent ligand for the translocator protein (18 kDa) in animal models of post-traumatic stress disorder. *Int. J. Neuropsychopharmacol.* **17**, 1659–69 (2014).
21. Wolf, L. *et al.* Enhancing neurosteroid synthesis—relationship to the pharmacology of translocator protein (18 kDa) (TSPO) ligands and benzodiazepines. *Pharmacopsychiatry* **48**, 72–77 (2015).
22. Scarf, A. M., Auman, K. M. & Kassiou, M. Is there any correlation between binding and functional effects at the translocator protein (TSPO) (18 kDa)? *Curr. Mol. Med.* **12**, 387–397 (2012).
23. Morohaku, K. *et al.* Translocator protein/peripheral benzodiazepine receptor is not required for steroid hormone biosynthesis. *Endocrinology* **155**, 89–97 (2014).
24. Tu, L. N. *et al.* Peripheral benzodiazepine receptor/translocator protein global knock-out mice are viable with no effects on steroid hormone biosynthesis. *J. Biol. Chem.* **289**, 27444–27454 (2014).
25. Copeland, R. A. Conformational adaptation in drug-target interactions and residence time. *Future. Med. Chem.* **3**, 1491–1501 (2011).
26. Mollica, L. *et al.* Kinetics of protein-ligand unbinding via smoothed potential molecular dynamics simulations. *Sci. Rep.* **5**, 11539 (2015).
27. Primofiore, G. *et al.* N,N-dialkyl-2-phenylindol-3-ylglyoxylamides. A new class of potent and selective ligands at the peripheral benzodiazepine receptor. *J. Med. Chem.* **47**, 1852–1855 (2004).
28. Da Settimo, F. *et al.* Anxiolytic-like Effects of N,N-Dialkyl-2-phenylindol-3-ylglyoxylamides by Modulation of Translocator Protein Promoting Neurosteroid Biosynthesis. *J. Med. Chem.* **51**, 5798–5806 (2008).
29. Barresi, E. *et al.* Deepening the Topology of the Translocator Protein Binding Site by Novel N,N-Dialkyl-2-aryindol-3-ylglyoxylamides. *J. Med. Chem.* **58**, 6081–6092 (2015).
30. Costa, B. *et al.* Anxiolytic properties of a 2-phenylindolglyoxylamide TSPO ligand: Stimulation of *in vitro* neurosteroid production affecting GABA<sub>A</sub> receptor activity. *Psychoneuroendocrinology* **36**, 463–472 (2011).
31. Simorini, F. *et al.* Medicinal chemistry of indolylglyoxylamide TSPO high affinity ligands with anxiolytic-like effects. *Curr. Top. Med. Chem.* **12**, 333–351 (2012).
32. Motulsky, H. J. & Mahan, L. C. The kinetics of competitive radioligand binding predicted by the law of mass action. *Mol. Pharmacol.* **25**, 1–9 (1984).
33. Sykes, D. A., Dowling, M. R. & Charlton, S. J. Exploring the mechanism of agonist efficacy: a relationship between efficacy and agonist dissociation rate at the muscarinic M3 receptor. *Mol. Pharmacol.* **76**, 543–551 (2009).
34. Guo, D., Mulder-Krieger, T., IJzerman, A. P. & Heitman, L. H. Functional efficacy of adenosine A2A receptor agonists is positively correlated to their receptor residence time. *Br. J. Pharmacol.* **166**, 1846–1859 (2012).
35. Louvel, J. *et al.* Agonists for the Adenosine A1 Receptor with Tunable Residence Time. A Case for Nonribose 4-Amino-6-aryl-5-cyano-2-thiopyrimidines. *J. Med. Chem.* **57**, 3213–3222 (2014).
36. Butlen, D. Benzodiazepine receptors along the nephron: [<sup>3</sup>H]PK 11195 binding in rat tubules. *FEBS Lett.* **169**, 138–142 (1984).
37. Olson, J. M. M., Ciliax, B. J., Mandril, W. R. & Young A. B. Presence of peripheral-type benzodiazepine binding sites on human erythrocyte membranes. *Eur. J. Pharmacol.* **152**, 47–53 (1988).
38. Hill, A. V. The mode of action of nicotine and curari, determined by the form of the contraction curve and the method of temperature coefficients. *J. Physiol.* **39**, 361–373 (1909).
39. Motulsky, H. & Christopoulos, A. Analyzing kinetic binding data. In: *Fitting models to biological data using linear and nonlinear regression. A practical guide to curve fitting*. New-York: Oxford University Press. 245–251 (2003 Eds).
40. Mukhin, A. G., Papadopoulos, V., Costa, E. & Krueger, K. E. Mitochondrial benzodiazepine receptors regulate steroid biosynthesis. *Proc. Natl. Acad. Sci. USA* **86**, 9813–9816 (1989).
41. Papadopoulos, V., Mukhin, A. G., Costa, E. & Krueger, K. E. The peripheral-type benzodiazepine receptor is functionally linked to Leydig cell steroidogenesis. *J. Biol. Chem.* **265**, 3772–3779 (1990).
42. Kozykowski, A. P. *et al.* Chemistry, binding affinities, and behavioral properties of a new class of “antineophobic” mitochondrial DBI receptor complex (mDRC) ligands. *J. Med. Chem.* **36**, 2908–2920 (1993).
43. Fallahi-Sichani, M., Honarnejad, S., Heiser, L. M., Gray, J. W. & Sorger, P. K. Metrics other than potency reveal systematic variation in responses to cancer drugs. *Nat. Chem. Biol.* **9**, 708–714 (2013).
44. Casarosa, P. *et al.* Functional and biochemical rationale for 24 h-long duration of action of olodaterol. *J. Pharmacol. Exp. Ther.* **337**, 600–609 (2011).
45. Bernassau, J. M., Reversat, J. L., Ferrara, P., Caput, D. & Lefur, G. A 3D model of the peripheral benzodiazepine receptor and its implication in intra mitochondrial cholesterol transport. *J. Mol. Graph.* **11**, 236–244 (1993).
46. Anzini, M. *et al.* Mapping and fitting the peripheral benzodiazepine receptor binding site by carboxamide derivatives. Comparison of different approaches to quantitative ligand-receptor interaction modeling. *J. Med. Chem.* **44**, 1134–1150 (2001).
47. Jaremko, L., Jaremko, M., Giller, K., Becker, S. & Zweckstetter, M. Structure of the mitochondrial translocator protein in complex with a diagnostic ligand. *Science* **343**, 1363–1366 (2014).
48. Nguyen, N. *et al.* Efficacy of etifoxine compared to lorazepam monotherapy in the treatment of patients with adjustment disorders with anxiety: a double-blind controlled study in general practice. *Human. Psychopharmacology* **21**, 139–149 (2006).
49. Rupprecht, R. *et al.* Translocator protein (18 kDa) as target for anxiolytics without benzodiazepine-like side effects. *Science* **325**, 490–493 (2009).
50. Rágo, L. *et al.* The effect of chronic treatment with peripheral benzodiazepine receptor ligands on behavior and GABA<sub>A</sub>/benzodiazepine receptors in rat. *Naunyn. Schmiedebergs. Arch. Pharmacol.* **346**, 432–436 (1992).
51. Chelli, B. *et al.* PK 11195 differentially affects cell survival in human wild-type and 18 kDa Translocator protein-silenced ADF astrocytoma cells. *J. Cell. Biochem.* **105**, 712–723 (2008).
52. Bradford, M. M. A rapid and sensitive method for the quantitation of microgram quantities of protein utilizing the principle of protein-dye binding. *Anal. Biochem.* **7**, 248–254 (1976).
53. Cheng, Y. & Prusoff, W. H. Relationship between constant (K<sub>i</sub>) and the concentration of inhibitor which causes 50% inhibition (IC<sub>50</sub>) of an enzymatic reaction. *Biochem. Pharmacol.* **22**, 3099–3108 (1973).

## Acknowledgements

Funding for this study was provided by the Italian Ministry of University and Scientific Research (PRIN-prot. 20098SJX4F; PRIN-prot. 2010W7YRLZ\_005 and FIRB-prot. RBFR10ZJQT\_002).

### Author Contributions

B.C. conceived and conducted the experiments, analyzed the results, wrote the manuscript. E.D.P. conceived and conducted the experiments, analyzed the results. C.G. conducted the experiments. E.B. synthesized TSPO ligands, performed the  $^1\text{H}$  NMR and elemental analyses. T.S. and F.D.S. revised the manuscript. C.M. conceived the idea of the manuscript and revised the manuscript.

### Additional Information

**Competing financial interests:** The authors declare no competing financial interests.

**How to cite this article:** Costa, B. *et al.* TSPO ligand residence time: a new parameter to predict compound neurosteroidogenic efficacy. *Sci. Rep.* **6**, 18164; doi: 10.1038/srep18164 (2016).



This work is licensed under a Creative Commons Attribution 4.0 International License. The images or other third party material in this article are included in the article's Creative Commons license, unless indicated otherwise in the credit line; if the material is not included under the Creative Commons license, users will need to obtain permission from the license holder to reproduce the material. To view a copy of this license, visit <http://creativecommons.org/licenses/by/4.0/>